CrossMark

Development of Gravity Theories in the View of TRAPPIST-1e

Nan Wang[1,2,5] , Lu-Yao Lu[1], Hui-Gen Liu[2,3], An-Dong Chen[2,3], Tiger Lu[4], Ao-Ran Cui[6], and Jun-Kai Wang[7]

[1] Marine Science and Technology College, Zhejiang Ocean University, Zhoushan 316022, China; wangnan@zjou.edu.cn
[2] Key Laboratory of Modern Astronomy and Astrophysics, Ministry of Education, Nanjing 210023, China; huigen@nju.edu.cn
[3] School of Astronomy and Space Science, Nanjing University, Nanjing 210023, China
[4] Department of Astronomy, Yale University, 219 Prospect, New Haven, CT 06511, USA
[5] Zhoushan Astronomical Society, Zhoushan 316000, China
[6] Kuang Yaming Honors School, Nanjing University, Nanjing 210023, China
[7] School of Physics, Nanjing University, Nanjing 210023, China

Abstract

Contrary to the solar system, most exoplanet systems detected hitherto are close-in and compact. One typical system is TRAPPIST-1, which has seven nearly co-planar terrestrial planets all within the orbit of Mercury, including three in the habitable zone. To evaluate the differences in developing sophisticated gravity theories from the solar system, we use *N*-body integrations to simulate ephemeris and reproduce some important astronomy phenomena observed on the potentially habitable planet TRAPPIST-1e. Retrograde motions of other planets last 1–2 orders of magnitude shorter than in the solar system, but occur much more frequently. Transit events of all inner planets can be observed steadily. Except for Kepler's first law, which is hard to notice for low eccentricities of planets, the other two laws can then be precisely verified in 10^2 days, because the areas swept by planets vary by $\lesssim 0.01\%$ and the observed semimajor axes and periods result in constants with theoretical and observation accuracies both $\lesssim 2\%$. However, the mean motion correlation implies that the Great Inequality is not always apparent between one pair of planets like Jupiter and Saturn. Furthermore, general relativity can hardly be discovered because it gives rise to perihelion precession of inner planets only ~0.1% of gravity precession, dozens of times smaller than Mercury. Our results support the possibility of developing part of gravity theories by potential exo-civilizations in compact systems like TRAPPIST-1.

Key words: planets and satellites: terrestrial planets – extraterrestrial intelligence – ephemerides – gravitation

1. Introduction

The field of astronomy plays an important role in understanding the universe, discovering physical laws, and validating these laws in extreme scales. To understand the solar system, in the 3rd century BC Eratosthenes calculated the perimeter of the Earth by using the difference of the solar radiation angle from two different sites. In the 15th century, the retrograde motion of Mars inspired Copernicus' heliocentric theory (Copernicus 1543), and this hypothesis explained the phenomenon well without the need for the complex epicycles from Ptolemy's geocentric theory.

After the medieval period, scientists like Galileo started to use telescopes to observe the night sky with high precision, leading astronomy to a modern era. Then gravitational theory was extensively developed by understanding celestial motion in the following centuries. Based on accurate solar system motion data from Tycho Brahe, Kepler derived three well-known planetary motion laws in Astronomia nova (Kepler 1609) and Harmonices mundi (Kepler et al. 1619). These became the base stones of gravitational theories, i.e., Newtonian mechanics (Newton 1687), as well as celestial mechanics. After the discovery of Uranus by

Herschel & Watson (1781), Adams and Le Verrier predicted the motion of Neptune from the O-C deviations in Uranus orbit (Adams 1846; Le Verrier 1846a, 1846b), which is a remarkable example of the successful application of Newtonian mechanics.

By the 20th century, with the development of physics and high-precision astronomical observations, accounting for the theory of relativity has become more and more important in astronomy, as opposed to pure Newtonian mechanics. E.g., general relativity (Einstein 1915) precisely predicts the perihelion precession of Mercury (Nobili & Will 1986), and provides a theoretical basis for studying black holes, dark matter, and many other astronomical objects in extreme conditions.

It can be seen that the observation of the major planets in the solar system has played a vital role in the history of understanding gravity theory. According to statistics from the NASA Exoplanet Archive, more than 5000 exoplanets have been detected until 2022 December, and over 5000 candidates await confirmation.[8] Space telescopes such as Kepler (Borucki et al. 2010) and TESS (Ricker et al. 2015) have discovered over 1000 planets with radii below two Earth radii, including dozens

---

[8] https://exoplanetarchive.ipac.caltech.edu/index.html

of temperate terrestrial planets (Hill et al. 2023). Recently, the Closeby Habitable Exoplanet Survey (CHES) mission has been proposed to discover habitable-zone Earth-like planets of the nearby solar-type stars (Ji et al. 2022). The possibility of civilizations on these planets has long been an attractive topic for human beings. If there are intelligent creatures on other planets, can they discover gravity theory from observations in their own "solar system," as human beings have done?

Until now, exoplanet systems show many differences when compared to the solar system. Due to observational selection bias, most planets in the habitable zone (hereafter HZ) are detected around M-type stars, since these stars have a much closer HZ than the solar system. These exoplanets are usually in compact systems and most of them are rocky planets in similar sizes (Weiss et al. 2018; Otegi et al. 2021). Multiple planet systems around M dwarfs are common, and the gravitational perturbations in such systems are usually stronger than those of the solar system because of the compact architectures and small mass of M-type dwarfs. How these stronger perturbations in such systems influence planetary motion, and whether the ephemerides of other planets deviate from Kepler's laws, are crucial for the civilizations on habitable planets to discover and understand gravity theory. Our motivation is to check the difficulty of discovering gravity theory for civilizations around M-type dwarfs via the same methods as humans, and test precision comparing with historical data on Earth.

As an extreme example, the TRAPPIST-1 system has seven terrestrial planets, including three in the HZ. The star, TRAPPIST-1, is a cool red dwarf and was found by Two Micron All-Sky Survey (2MASS) in 1999 (Gizis et al. 2000). In 2017, Transiting Planets and Planetesimals Small Telescope (TRAPPIST, Jehin et al. 2011) discovered seven planets (b~h) orbiting around TRAPPIST-1 (Gillon et al. 2017). The longest period of the outermost planet h is about 19 days (Agol et al. 2021), which is even shorter than Mercury's period. The masses of the seven Earth-like planets are not well determined, and the planetary system may be unstable dynamically in some cases (Luger et al. 2017). Thus, the TRAPPIST-1 system is more compact and dynamically perturbed compared with the solar system. The formation of such a compact and flat system has been studied by lots of previous works (Tamayo et al. 2017; Schoonenberg et al. 2019; Heising et al. 2021; Izidoro et al. 2021). It is speculated that planets e, f, and g are located in the habitable zone, hence with the probability of breeding civilization (Gillon et al. 2017).

In this paper, we focus on the TRAPPIST-1 system and choose planet e as a potentially habitable world. We simulate the planet ephemeris on the sky of planet e, based on an N-body numerical model. To understand planetary motion in the context of heliocentric theory in the TRAPPIST-1 system, we calculate the retrograde motions for other planets and the transit events of inner planets. We also test Kepler's Laws and general relativity via the planetary ephemeris. Comparing with

Table 1
The Orbital Parameters of the TRAPPIST-1 System at BJD = 2457257.931 and 5 kyr Later in Our Simulation

Planet	a (au)	T (days)	e	i (°)	ω (°)	f (°)
Initial Conditions						
b	0.01155	1.514	0.00306	89.728	134.735	45.982
c	0.01583	2.427	0.00055	89.778	1.042	351.431
d	0.02229	4.057	0.00563	89.896	151.706	15.062
e	0.02930	6.110	0.00633	89.793	313.206	142.898
f	0.03855	9.220	0.00842	89.740	183.474	300.029
g	0.04689	12.370	0.00401	89.742	18.616	77.695
h	0.06198	18.798	0.00365	89.805	180.314	69.320
5000 yrs later						
Planet	a (au)	T (days)	e	i (°)	ω (°)	f (°)
b	0.01155	1.513	0.00446	89.719	319.452	131.664
c	0.01583	2.427	0.00144	89.774	141.255	324.767
d	0.02230	4.058	0.02650	89.852	231.395	295.413
e	0.02932	6.115	0.01645	89.741	316.746	90.010
f	0.03852	9.222	0.01966	89.771	122.907	260.695
g	0.04691	12.382	0.00617	89.782	280.999	40.675
h	0.06203	18.807	0.00418	89.720	225.540	162.064

ephemeris on Earth, we conclude how well gravity theory can be tested in the TRAPPIST-1 system.

This paper has four sections arranged as follows. In Section 2, we build up a numerical model and introduce the initial setups for TRAPPIST-1 system. In Section 3, we calculate the retrograde motions and transit events in the sky of TRAPPIST-1e. We also use the ephemeris to verify Kepler's Laws and evaluate the Great Inequality effect in Section 4. General relativity is tested via the orbital precession of inner planets in Section 5. Finally, we conclude our results and discuss the validation in Section 6.

2. Numerical Simulations of the TRAPPIST-1 System

In this section, we introduce how we integrate the planetary ephemeris in the TRAPPIST-1 system and the initial setups. We choose the REBOUND package for our N-body simulations to calculate ephemeris (Rein & Liu 2012). A 15th order Gauss-Radau integrator, IAS15 (Rein & Spiegel 2015), is used. We only consider the classic N-body Newtonian gravity to calculate the positions and motions of the seven planets.

The initial conditions of each planet, which include semimajor axis a, eccentricity e, inclination i, argument of pericenter ω, true anomaly f, mass M_p, and radius R_p, are adopted from Agol et al. (2021) at epoch of BJD = 2457257.931 as shown in Tables 1 and 2. The mass of the host star M_* is 8.98×10^{-2} solar masses (Mann et al. 2019). All the longitudes of ascending nodes are set as $0°$. Then we obtained the evolution of the orbital elements over the next 5000 Earth years (i.e., 3×10^5 orbital period of TRAPPIST-1e) and recorded outputs every 0.5 Earth days. Table 1 shows the

Table 2
The Constant Parameters of the TRAPPIST-1 System in Our Simulation

Planet	M_p ($M_\oplus$)	R_p ($R_\oplus$)
b	1.374	1.116
c	1.308	1.097
d	0.388	0.788
e	0.692	0.920
f	1.039	1.045
g	1.321	1.129
h	0.326	0.755

Table 3
The Hill Radius R_H and the Separation Factor K Between Planets in the Solar System and the TRAPPIST-1 System

Solar System	R_H (au)	K
Average	…	25.96
Venus–Mercury	0.00530	63.40
Earth–Venus	0.0105	26.31
Mars–Earth	0.0131	40.10
Jupiter–Mars	0.230	16.02
Saturn–Jupiter	0.549	7.89
Uranus–Saturn	0.688	14.03
Neptune–Uranus	0.780	13.95
TRAPPIST-1	R_H (au)	K
Average	…	10.31
b-c	0.000425	10.05
c-d	0.000508	12.74
d-e	0.000591	11.85
e-f	0.000910	10.17
f-g	0.001271	6.57
g-h	0.001436	10.51

orbital elements of all planets after 5 kyr. Given the positions and velocities of the seven planets, we transform them into the horizontal coordinates of TRAPPIST-1 e (Section 3). Based on the horizontal coordinates, we can study the ephemeris observed from TRAPPIST-1e. In addition, the sidereal period T is calculated according to the evolution of the orbital elements and is used to test Kepler's laws and the Great Inequality (Section 4).

Even 5 kyr is already comparable to the time humans developed gravity theories, there is a concern that the initial conditions may lead to long-term instability after the early stable evolutions analyzed in this work, because of the system's compactness and active resonances. To qualify the compactness of the TRAPPIST-1 system, we check the separation of planet pairs in the system by using the Hill radius defined by Chambers et al. (1996)

$$R_H = \frac{a_1 + a_2}{2} \cdot \left(\frac{M_1 + M_2}{3M_*}\right)^{1/3} \quad (1)$$

and the separation factor $K = |a_1 - a_2|/R_H$, where a_1 and a_2 represent the semimajor axes of two planets, M_1 and M_2 represent the masses of two planets. The smaller the separation scaled by R_H is, the more compact these two planets are. Here we use the semimajor axes of the planets of the TRAPPIST-1 system in Table 1. As shown in Table 3, the average separation in the TRAPPIST-1 system is ~10.3R_H, while the most compact planet pair is f and g, with a separation of 6.6R_H. Compared to the inner solar system, the TRAPPIST-1 system is 3~6 times more compact. According to the empirical relationship between K and stability (Volk & Malhotra 2020), TRAPPIST-1 should be marginally stable. In addition, the resonance ratio of the seven planets forms a long resonance chain: 24:15:9:6:4:3 (Luger et al. 2017). The diversity of the resonances shows the complexity of this extra-terrestrial compact planet system. However, if convergent migration happens, the TRAPPIST-1 system can still be stable on a timescale of ~10^7 yr (Tamayo et al. 2017).

Our early evolutions are shown in Figure 1. The oscillating patterns of eccentricity, inclination and pericenter of each planet are illustrated. The seven planets are on a common plane

inclined at about 89°.8 with a maximum deviation of no more than 0°.3. Thus, compared with the solar system the TRAPPIST-1 system is more co-planar. The eccentricity of the planet e, oscillating between 0 and 0.03, is similar to that of Earth. Pericenter precession can be seen on each planet of the system, which will be discussed more in Section 5. We further lengthen the simulation time and compare the evolutions after 1 Myr with the early evolutions to clarify the long-term stability. Figure 2 shows that even under gravitational perturbations the semimajor axes of the seven planets nearly remain the same as the initial values without irregular jumps. The eccentricities still oscillate, but by the magnitudes close to the early evolutions, and the oscillation of planet e is 0.017, even smaller than the early one. Therefore, we point out that some values of eccentricities 5 kyr later in Table 1 seem to obviously increase during the simulation, which can mislead to an instability of the system with excited orbits. However, those values at merely one instant are contributed by the oscillations, which are no stronger even after 1 Myr than the early evolutions. Briefly, though the orbital elements' evolutions contain periodic signals (Figure 1), the stability of the TRAPPIST-1 system over the timescale of 5 kyr is certain.

Based on the time series of seven planets, we mimic virtual observations from TRAPPSIT-1e and produce the celestial ephemeris that would be seen from the planet. In the next section, we will investigate the retrograde motions and transits of the inner planets in the TRAPPIST-1 system.

3. The Observation of Retrograde Motion and Transit

On Earth, retrograde motions of Mercury, Venus, and Mars have been observed. In fact, Martian retrograde motion is what
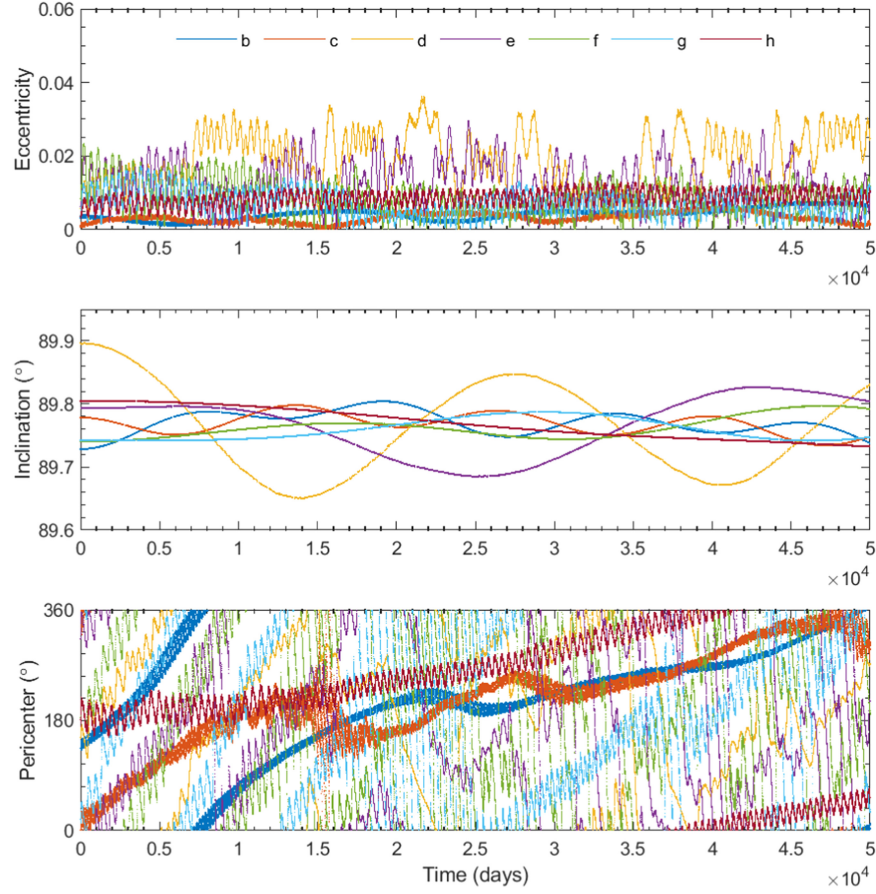
Figure 1. Evolutions of eccentricity, inclination and argument of pericenter of planets in the TRAPPIST-1 system in 50,000 days from 2457257.931 BJD.
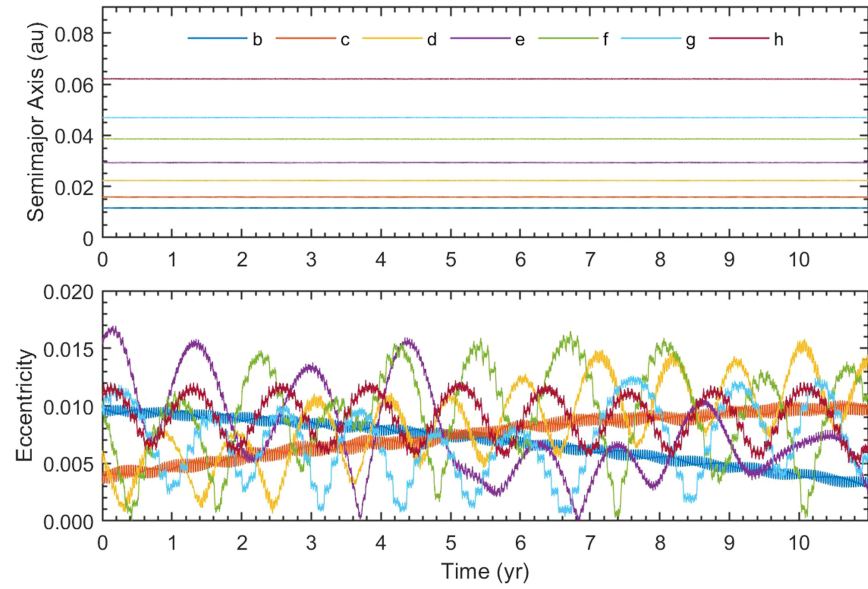

Figure 2. Evolutions of semimajor and eccentricity of planets in the TRAPPIST-1 system in 10 yr after 1 Myr later.
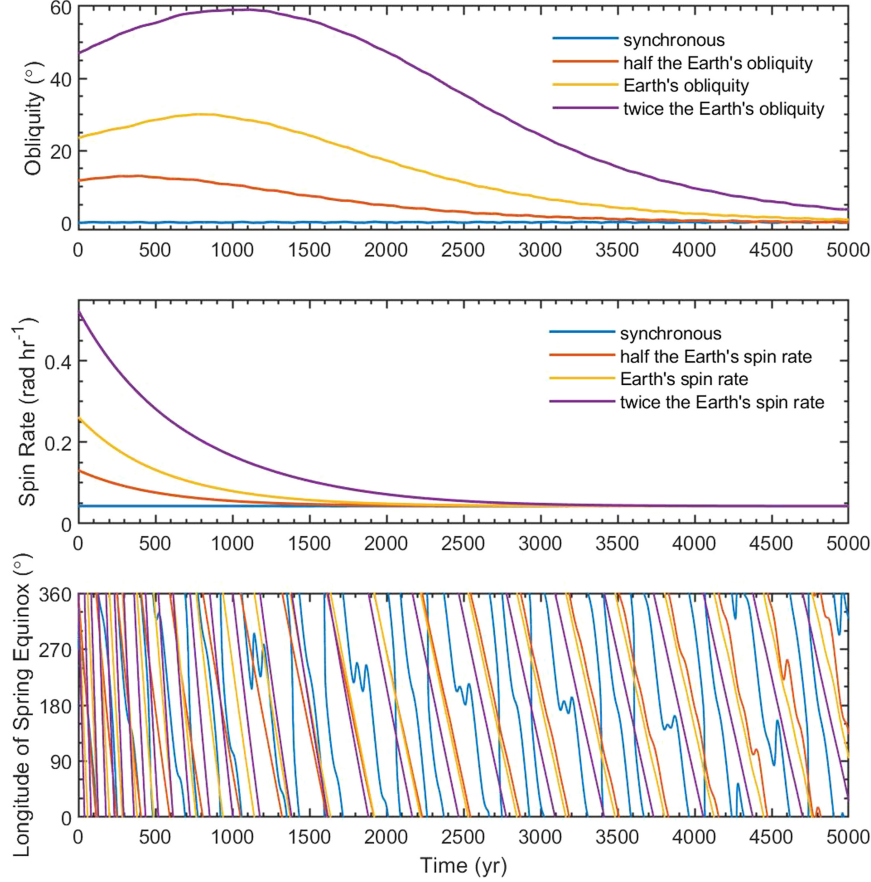
Figure 3. Evolutions of obliquity, spin rate, and longitude of spring equinox of TRAPPIST-1e in 5 kyr from 2457257.931 BJD. The blue curve represents the case that the planet is set synchronous at the initial instant. The red, yellow and purple ones represent the cases that the planet is initially set with half, equal and twice the spin parameters of Earth, respectively (except that the longitude of spring equinox is 0° initially in all the cases).

caused Copernicus to become suspicious of geocentric theory and hence establish heliocentric theory, starting a new era of astronomical exploration. In addition, transits of the inner planets, an important phenomenon that once helped humans recognize the scale of the solar system, are also studied in this section to characterize the TRAPPIST-1 system. Hereafter, we will inspect the synchronous status and the habitability of TRAPPIST-1e, and then search and study the occurrence of those two important phenomena in the sky of TRAPPIST-1e.

3.1. Spin Evolution and Insolation Distribution of TRAPPIST-1e

To derive the virtual observation from TRAPPIST-1e, the astrocentric coordinates of the system need to be transformed into the horizontal coordinates of TRAPPIST-1e, so its spin evolution needs to be known. According to the simulations of Bolmont et al. (2015), an Earth-mass planet orbiting a 0.08 $M_{\odot}$ host evolves toward synchronization in less than 2×10^3 yr,

indicating a similar damping timescale for TRAPPIST-1e. We confirm that by comparing four simulations with the same initial conditions (Table 1), except that planet e is synchronous with obliquity $\varepsilon = 0°$ in the first case but has various spin rates and obliquities (half, equal and twice the values of Earth) in the other cases. To track the spin evolution of the planet, we use the tides_spin implementation of equilibrium tide theory (Eggleton et al. 1998; Lu et al. 2023) which is included in the REBOUNDx package of add-ons (Tamayo et al. 2020). Figure 3 shows that the spin rate and obliquity damp fast to synchronization even the planet e is initially non-synchronous, so it is reasonable to assume that planet e has long been synchronous at the initial date of the simulation. Then the first case where planet e has reached the synchronization from the beginning is used to derive the virtual observation and subsequent analyses.

Starting from the initial synchronous status, planet e remains synchronous through the following 5 kyr (Figure 3). Still, to

obtain precise projected positions of other planets, we consider the precession and nutation of the spin axis of TRAPPIST-1e, due to perturbations from other planets. According to the simulation results shown in Figure 3, the precession period of planet e is about 278 yr, and its nutation period is about 227 yr with a variation of ε no more than $0°\!.8$. Both of those periods are much longer than the timescale of the phenomenon discussed in Section 3, so the precession and nutation of TRAPPIST-1e should not affect observations from the planet. The precession effects due to tides and general relativity are taken into account in Section 5 to evaluate the possibility of discovering general relativity theory.

We further investigate the insolation distribution of TRAPPIST-1e given its spin evolution to assess its habitability. The mean insolation of one revolution can be estimated analytically with the elliptic integral method adopted from Wang & He (2019). The insolation W depends on the planet's semimajor axis, eccentricity, obliquity as well as the host star's luminosity L_*.

Figure 4. Insolation distribution of TRAPPIST-1e compared to Earth. The dashed lines bound the overlapped insolation range of two planets.

the peak of a flare of M dwarfs, the ultraviolet radiation received by Earth-like planets within HZs would exceed the level received by Earth for only some minutes. Additionally, although ozone depletion can be induced by protons, it is

$$
W = \begin{cases}
\frac{L_*\cos\varphi}{2\pi^3 a^2 \sqrt{1-e^2}}\left[E\left(\frac{\sin\varepsilon}{\cos\varphi}\right) + \tan^2\varphi K\left(\frac{\sin\varepsilon}{\cos\varphi}\right) - \tan^2\varphi\cos^2\varepsilon \Pi\left(\sin^2\varepsilon, \frac{\sin\varepsilon}{\cos\varphi}\right)\right], & |\varphi| < |90° - \varepsilon| \\[2ex]
\frac{L_*\sin\varepsilon}{2\pi^3 a^2 \sqrt{1-e^2}}\left[E\left(\frac{\cos\varphi}{\sin\varepsilon}\right) + \cot^2\varepsilon K\left(\frac{\cos\varphi}{\sin\varepsilon}\right) - \sin^2\varphi\cot^2\varepsilon \Pi\left(\cos^2\varphi, \frac{\cos\varphi}{\sin\varepsilon}\right)\right], & |\varphi| > |90° - \varepsilon| \\[2ex]
\frac{L_*}{2\pi^3 a^2 \sqrt{1-e^2}}[\sin\varepsilon + \cos^2\varepsilon \, \mathrm{arctanh}(\sin\varepsilon)], & |\varphi| = |90° - \varepsilon|
\end{cases}
\tag{2}
$$

where E, K, Π are the first, second and third complete elliptic integrals, respectively. Using the simulated parameter values of TRAPPIST-1e and $L_* = 0.000553 L_\odot$ (Ducrot et al. 2020), the insolation distribution is obtained as shown in Figure 4. The insolation of TRAPPIST-1e has a similar latitudinal trend with Earth, i.e., a convex shape with one peak at the equator and two equal bottoms at the poles, because of its small obliquity. The value of insolation of TRAPPIST-1e is smaller than that of Earth at each latitude, but comparable in general. The latitudes lower than $52°$ on TRAPPIST-1e overlap the latitudes higher than $51°$ on Earth, where the insolation ranges between 173 and $281\,\mathrm{W\,m^{-2}}$. As the orbit and obliquity of TRAPPIST-1e evolves, its insolation varies by only 0.7% in 5 kyr. Given the insolation is suitable and stable, it can also be easy to satisfy the heat transport efficiency to maintain the global atmosphere of tidally locked planets (Joshi 2003). Thus, there should be no obstacles to the habitability of TRAPPIST-1e, in terms of its insolation and synchronous status.

Nevertheless, as an M dwarf, the stellar activity of TRAPPIST-1 may be considered disadvantageous to habitability. Simulations of Segura et al. (2010) showed that even at
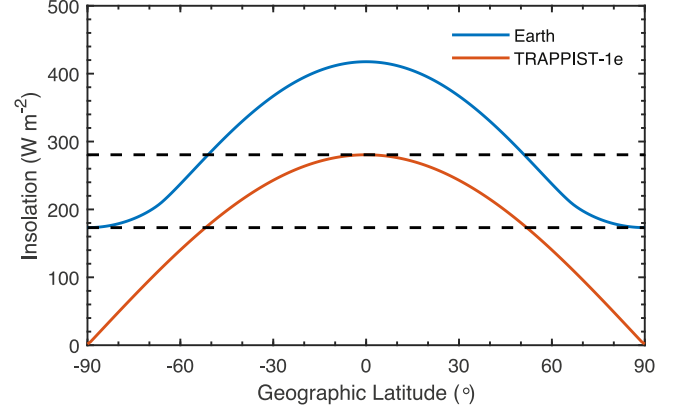
temporal and recoverable. In other words, a single flare event has no permanent hazard on habitability. Repeated flares can result in direct harm to life and comprehensive destruction of ozone shields (Tilley et al. 2019), but M dwarfs usually cool down after the initial ~1 Gyr, and the recovery of the planetary atmosphere during long-term evolution is achievable.

Considering factors including the insolation, the host's stellar activity and orbital stability (Wolf 2017; Dong et al. 2018), it can be assumed that during the simulation, TRAPPIST-1e has a stable and habitable environment for a civilization to make astronomical observations and develop theories.

3.2. Retrograde Motions Inspiring Heliocentric Theory

Retrograde motion is a basic and important phenomenon in the solar system. In Ptolemy's geocentric model, in order to satisfy both the motion of the star along its perfect circumference trajectory and the retrograde motions of planets, it is necessary to add the epicycles to the deferent and introduce a series of complex concepts such as eccentric and equant. The final "wheel-on-wheel" system can include more than 80
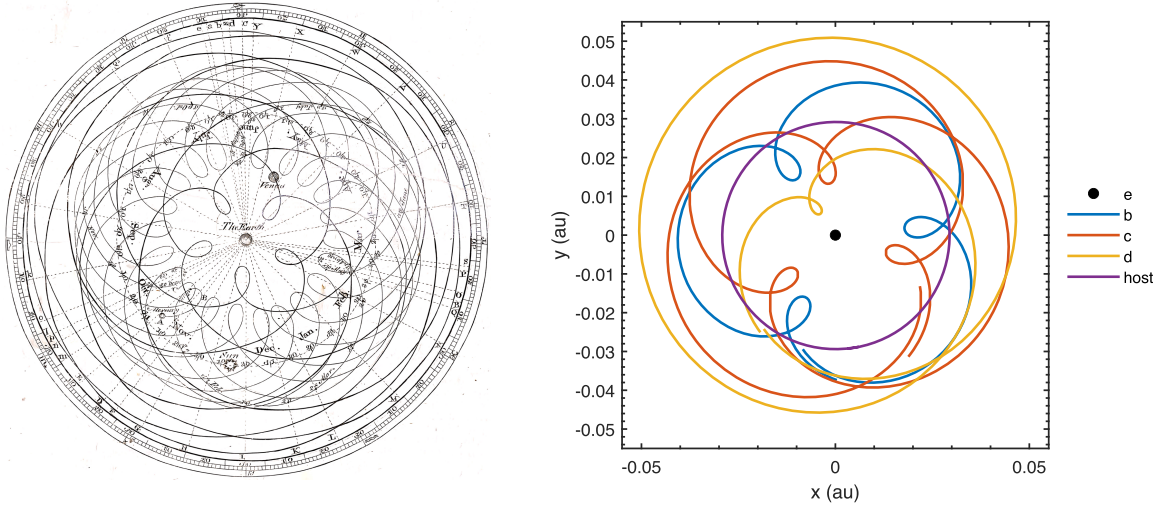
Figure 5. Similarity between the geocentric theory of the solar system (left, A Society of Gentlemen in Scotland 1771) and motions of planets seen from TRAPPIST-1e (right).

epicycles to a scale of affecting interplanetary motions, as shown in Figure 5. Because the interpretation of retrograde motion was too complex, Copernicus developed his heliocentric theory in response. After Copernicus introduced the heliocentric model, the epicycles of the planets were reduced to about 30. The sizes of the epicycles, although was still considered a perfect circumference, were reduced to very small extents. From then on, heliocentric theory began to be accepted and recognized by public at large.

Kepler then assumed that the planets were moving along elliptical orbits and eventually proposed Kepler's first law, based on the 8′ uncertainty in the orbital observations of Mars. It can be seen that the two important milestones in astronomy above are closely related to observations of retrograde motion, so therefore we are inspired to explore it in the TRAPPIST-1 system.

Based on the projected positions of other planets on the TRAPPIST-1e celestial sphere, we can draw their trajectories and observe if and when there is retrograde motion. While the astrocentric coordinates of the system are transformed into the horizontal coordinates of TRAPPIST-1e, the planet's spin evolution (Section 3.1) is considered. Note the annual parallax is considered automatically in the coordinate conversion. The typical retrograde motions are illustrated in Figure 6. We can obtain some features about the phenomenon of retrograde motions observed in the TRAPPIST-1 system and compare it with that observed on Earth. Since the durations and trajectories of retrograde motions vary from time to time, we have measured some quantitative characteristics of retrograde motions in the TRAPPIST-1 system in 500 days (~82 orbit periods of planet e), and the results are shown in Table 4 and Figure 7.

As we can see, in the solar system, the planets have longer durations and lower frequencies of retrograde motions, whereas the frequencies of retrograde motions in the TRAPPIST-1 system are significantly larger. The typical duration and interval in the latter system are both 1–2 orders of magnitude shorter than the former. These phenomena can be explained by the compactness of the TRAPPIST-1 system, i.e., a smaller orbital period leads to a shorter duration of retrograde motion, and a closer distance leads to a higher frequency of it. However, compared with Mercury and Mars, the ratios of total durations of all retrograde motions in a certain time to this time length for planets in TRAPPIST-1 are comparable and no more than double. Additionally, the arcs of retrograde motions in the two systems are quite close, i.e., the retrograde motion displacements in the sky are almost equally obvious. Hence, there should also be a good chance to notice this phenomenon in the TRAPPIST-1 system.

3.3. Transit Events Allowing Distance Measurements

Transits are important phenomena in understanding the absolute scale of the solar system. The first known attempt to determine the Sun–Earth distance with geometry was made by Aristarchus (Commandino 1572). Shortly after, Hipparchus realized that determining the Sun–Earth distance in the unit of Earth's radius was equivalent to determining the solar parallax (the angle between the line through the centers of Earth and the Sun and the tangent line touching the Earth's surface through the center of the Sun) (Toomer 1978). In the 17th century, benefiting from telescopic observations, Kepler limited the solar parallax to 1′, which corresponds to the Sun–Earth distance of 3469 Earth radii (Helden 1985). In the 18th century, Halley proposed to determine the solar parallax via
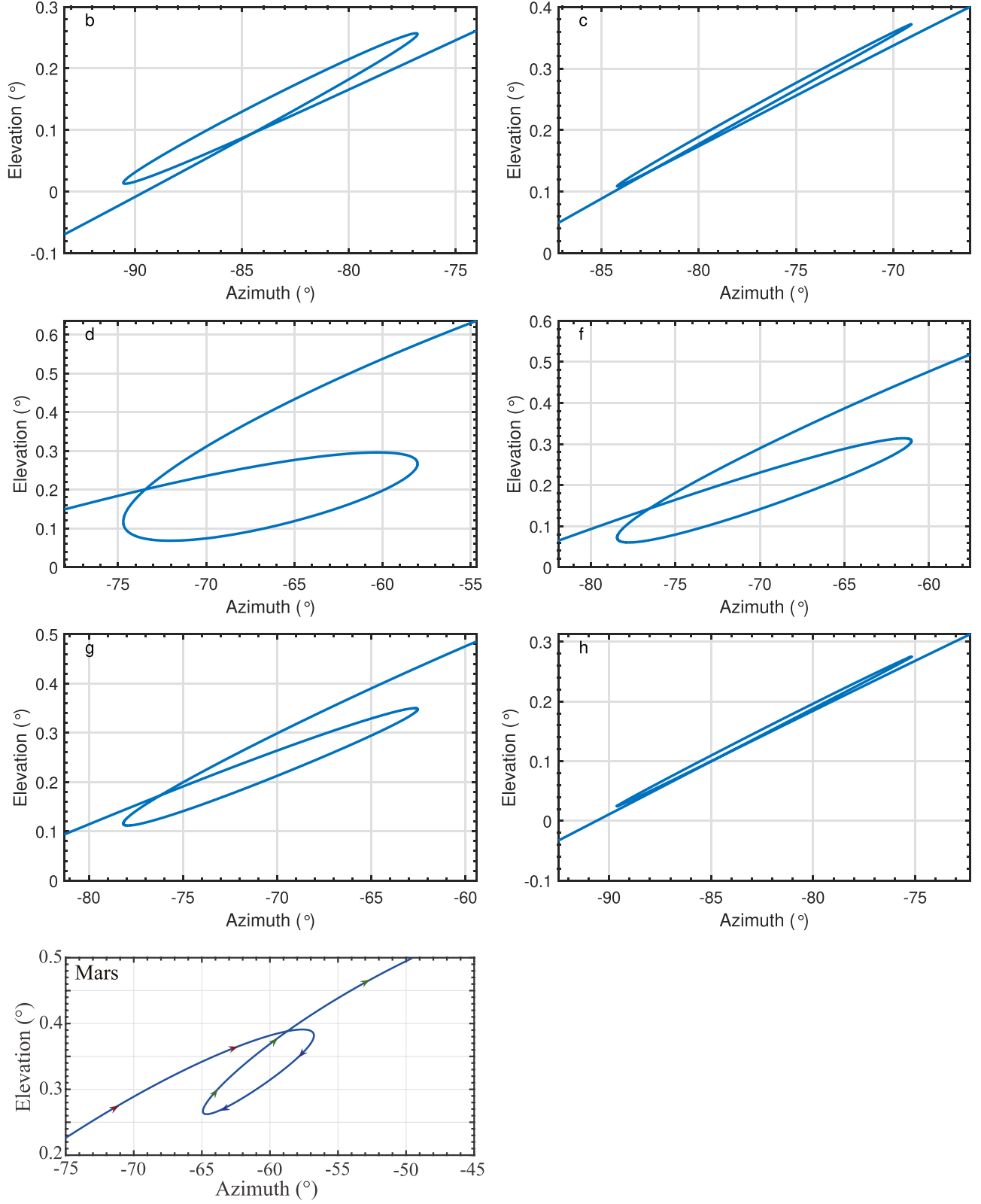
Figure 6. The retrograde motion trajectory of TRAPPIST-1b, c, d, f, g, h and Mars on the sky projection.
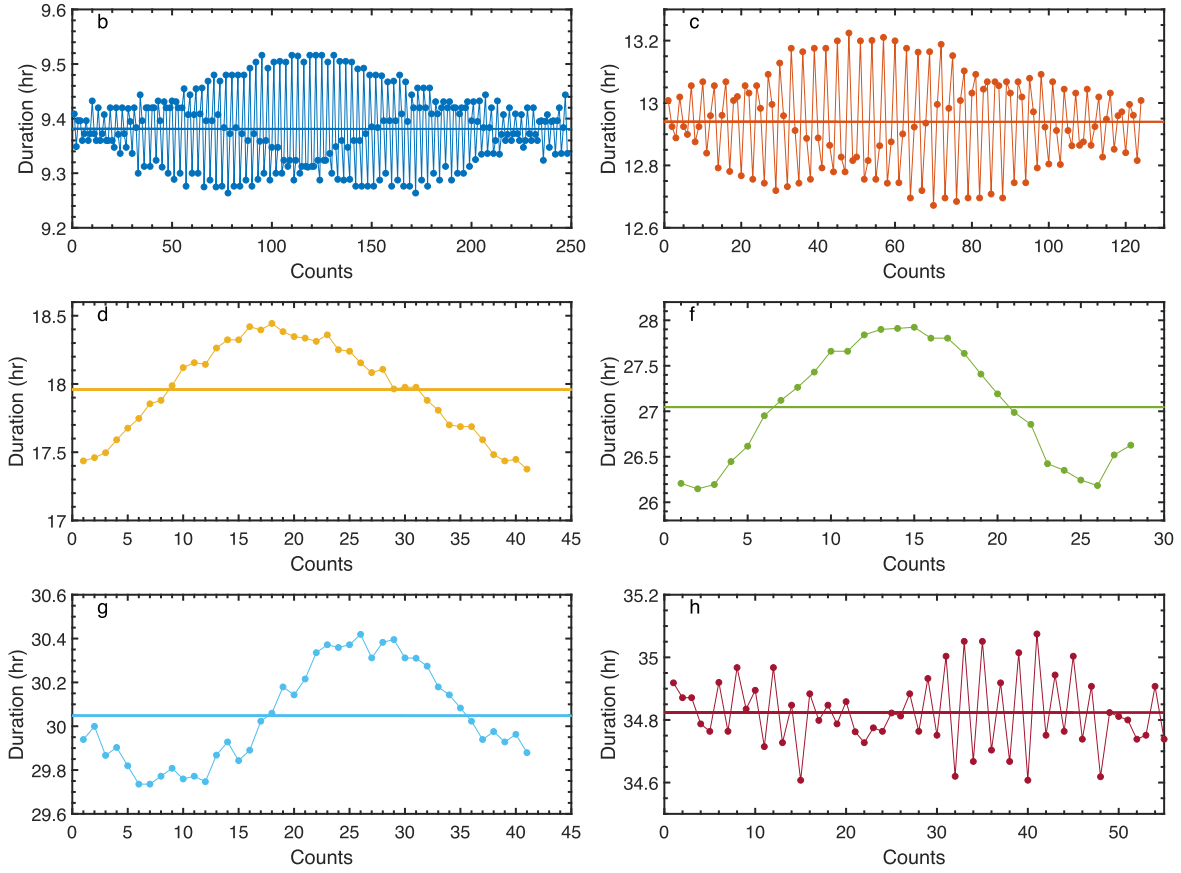
Figure 7. Durations of retrograde motions of TRAPPIST-1b, c, d, f, g and h seen from TRAPPIST-1e distributed in 500 days. The solid line represents the mean duration. Time starts from 2457257.931 BJD.

Table 4.
Comparison of Retrograde Motion Data from the TRAPPIST-1 System and the Solar System

	Arc (°)	Duration (days)	Interval (days)	Ratio
Mercury	13.2	21	118.8	15.0%
TRAPPIST1-b	13.9	0.39	1.62	19.4%
TRAPPIST1-c	15.3	0.54	3.49	13.4%
TRAPPIST1-d	17.1	0.75	11.33	6.2%
Mars	18.1	72	781.2	8.4%
TRAPPIST1-f	17.0	1.13	16.93	6.2%
TRAPPIST1-g	15.9	1.25	10.80	10.4%
TRAPPIST1-h	14.7	1.45	7.59	16.1%

Note. The first column is the angular distance of retrograde motion seen from TRAPPIST-1e or Earth. The second and third columns are the duration and interval of it, respectively. The fourth column is the ratio of the summed duration of all retrograde motions to total time.

observations of the transit of Venus (Halley 1716). In this method, the difference in the transit duration observed in different locations on Earth is compared to the expected difference calculated from an estimate of the solar parallax, so that the estimate can be effectively corrected (Browne 2005). After the international effort was undertaken to observe the 1761 and 1769 transits, the mean parallax was precisely determined to be 8″.78, leading to eight-tenths of a percent difference in the Sun–Earth distance (Hornsby 1771).

The same method can be used in the TRAPPIST-1 system, based on the transit timings of the inner planets, which would allow the possible extrasolar civilizations to calculate the distance from TRAPPIST-1e to their host star. From the perspective of a civilization on TRAPPIST-1e, we can model the trajectory of each inner planet and TRAPPIST-1 itself on the sky. The radius of TRAPPIST-1 is 0.1192 solar radius (Agol et al. 2021), leading to an apparent radius of about 1°.1. Transits are spotted when the angular distance between an inner planet and the host is smaller than the host's apparent radius. Some typical transits are shown in Figure 8. The transits of all three inner planets are obvious. In particular, simultaneous transits of double planets are not difficult to find. This is because the TRAPPIST-1 system is both more co-planar and compact than the solar system, and the apparent radius of
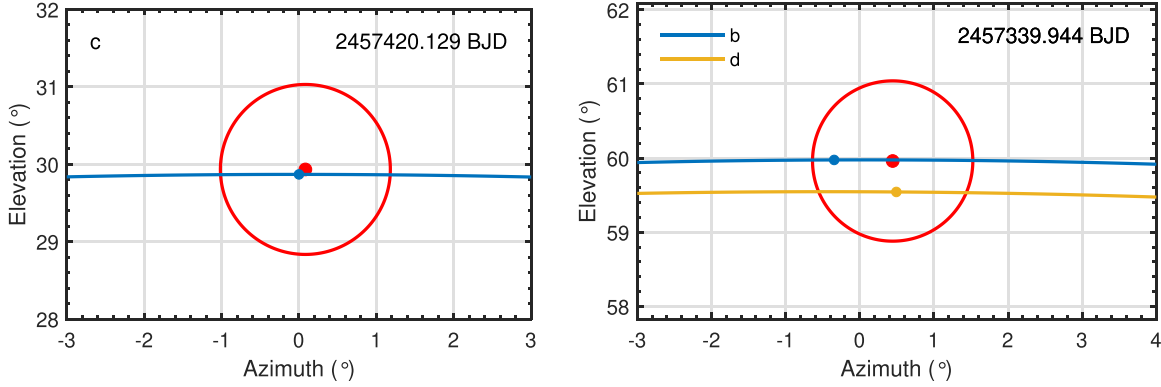
Figure 8. Transit of TRAPPIST-1 c observed at geometric latitude 60°N (left) and simultaneous transits of TRAPPIST-1b and TRAPPIST-1d observed at 30°N (right) on TRAPPIST-1e. The curves are the projected trajectories of inner planets, and the dots in the same colors indicate the locations of inner planets at the epoch of labeled BJD. The red dot and circle are the center and the rim of the host star at that epoch.
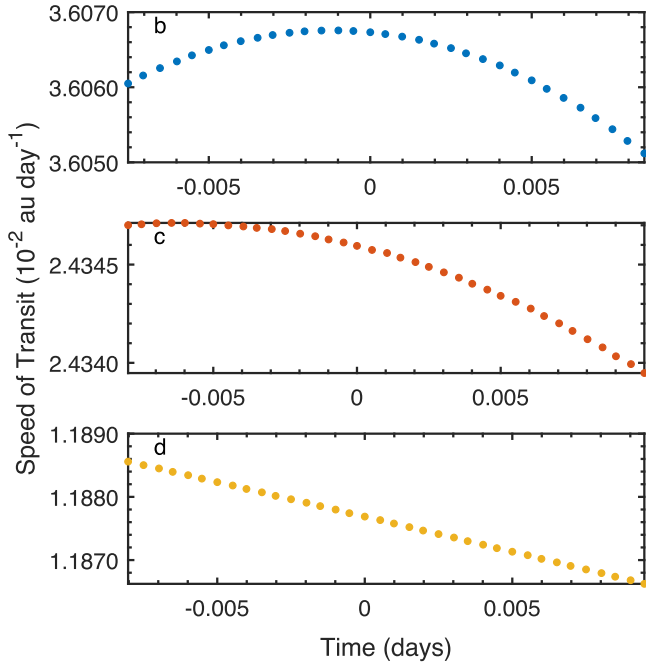

Figure 9. The speeds of TRAPPIST-1b, c, d during the transits shown in Figure 8. The time at zero-point is the moment of mid-transit, that is, BJD = 2457339.947 (b), 2457420.129 (c), 2457339.943 (d) in turn.

TRAPPIST-1 is much bigger than that of the Sun as seen from Earth (16′). These facts ensure that observed transits are not rare on TRAPPIST-1e.

It should be noticed that since the eccentricities of TRAPPIST-1b and TRAPPIST-1d can increase to greater than that of Venus, we need to estimate the speed during transit to ensure the speed can be considered as constant to calculate the distance between the host star and the planet. Our calculation confirms that the speed variation during the transit for planets b, c and d can all be neglected (Figure 9). During those transits, the speeds of planets

vary only $\lesssim 0.1\%$. Thus it can be assumed that the speeds of inner planets are constant during transits, and the distance calculation via trigonometric parallax is valid, assuming the transit duration is determined by the contact parameters. For comparison, the transit speed of Venus seen from Earth is about 8.3×10^{-3} au day^{-1}, and differs less than 1%.

Since we have simulated transit events in the TRAPPIST-1 system, the distance of TRAPPIST-1e to the host when a transit is observed can be calculated to be $R_{\rm e}/\sin\alpha$. To determine the horizontal stellar parallax of the host star α, Short's method (Short 1761, 1763) is implemented, as it was for the solar parallax with the collected data from observations of the 1761 transit of Venus. An initial estimate is set to be $\alpha_{\rm i} = 0\overset{''}{.}070$, smaller than the accurate value $0\overset{''}{.}077$ by an error of 9%, which is comparable to that of the $8\overset{''}{.}5$ hypothesis of solar parallax (Short 1763). The virtual observation of a transit of the closest planet, TRAPPIST-1d, is taken as an example. As seen from an observer at latitude 60°N on TRAPPIST-1e, this transit duration is observed to be $t_{\rm o} = 0.3837$ hr (the mid-transit happens at 2457738.602 BJD). Additionally, the theoretical duration for this observer calculated from $\alpha_{\rm i}$ is $t_{\rm th} = 0.3852$ hr and the theoretical duration as viewed from the center of TRAPPIST-1e is $t_{\rm c} = 0.4063$ hr. (This calculation process is detailed by Teets 2003) Thus, the proportion

$$\frac{\alpha_{\rm i}}{\alpha} = \frac{t_{\rm c} - t_{\rm th}}{t_{\rm c} - t_{\rm o}}. \tag{3}$$

yields $\alpha = 0.075$, equivalent to a distance from TRAPPIST-1e to the host being 0.02998 au, with a deviation from the accurate distance being 3%. Therefore, the absolute scale of the TRAPPIST-1 system can be determined via observations of transits.

4. The Test of Kepler's Laws of Planetary Motion

Both the phenomena of retrograde motions and transits in the TRAPPIST-1 system will help develop an understanding of heliocentric theory and assist in measuring the semimajor axes
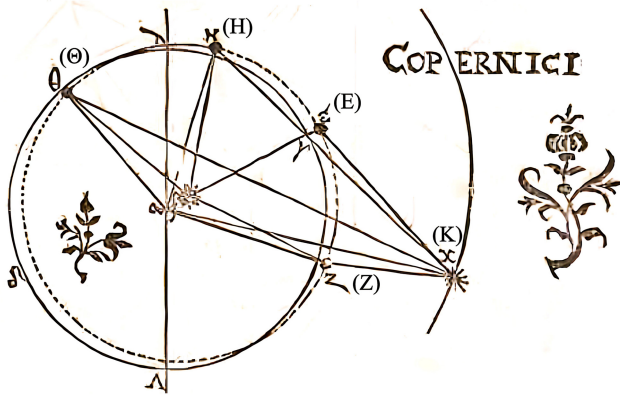
Figure 10. Johannes Kepler's triangulation method of determining Mars' orbital position described in Astronomia nova (Kepler 1609). Every 687 days, Mars returns to the same position K, but Earth starts at Θ and continues around to H after a complete counterclockwise evolution.

Figure 11. Constructed orbit of TRAPPIST-1f (green solid curve) by method of triangulation. The orbit of planet e (purple dashed curve) is assumed to be a circle. The green dashed curve is the accurate orbit of planet f. The gray dots are excluded from ellipse fitting.

of the planets. In this section, we will test the precision of Kepler's laws according to the simulated planetary ephemeris on TRAPPIST-1e.

4.1. Kepler's First Law

Kepler's first law states that planets' orbits are ellipses. Kepler first verified Mars' elliptical orbit with his ingenious method of triangulation in Astronomia nova (Kepler 1609). Before the method was implemented, Kepler knew that Mars' orbital period was 687 days, which could be determined with the recorded time between its successive oppositions (synodic period) as well as the Earth's orbital period, 365 days. Kepler then collected from Tycho's log books the apparent positions of Mars 687 days apart, when Mars was assumed to be at the same position in its orbit relative to the Sun but Earth was assumed not (Figure 10). The directions to Mars indicated by at least two of those observations from Earth in different positions along its assumed circular orbit led to one common intersection point, which was taken as one orbital position of Mars. To locate another orbital position of Mars, a series of observations every 687 days apart with another start date was used. Given the access to Martian data covering a couple of decades, Kepler triangulated several orbital positions of Mars. Thus, the motion trajectory of Mars was traced out and well fitted by an ellipse (with error reduced to 2′ in Rudolphine Tables (Kepler 1627)).

We determine the orbit of TRAPPIST-1f using the same method with the simulated ephemeris on TRAPPIST-1e (simulation in 500 days with an integration step of 1/2000 days). The orbit of planet e is assumed to be circular. Using each pair of data $T_f = 9.220$ days apart to triangulate just one position of planet f, ephemeris in two successive periods from 2457263.960 BJD results in the orbit constructed by connecting every triangulated position shown in Figure 11. The reason why a small portion of the whole orbit cannot be
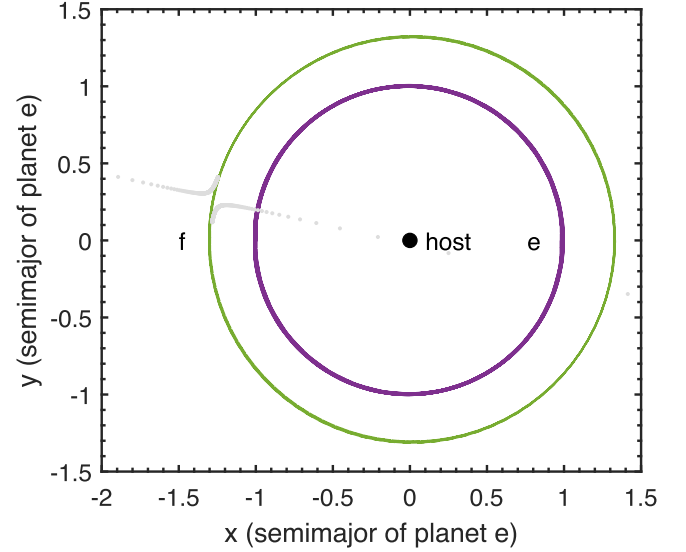
realistically constructed is the special proportion of orbital periods of planets e and f. Because $T_f/T_e = 1.5$, at the dates T_f apart, planet e is always in either one of two roughly opposite directions from the host. In addition, once either opposition or conjunction of planet f happens (the host and two planets are lined up), these two events occur in turn in this series of observations. Even the difficulty of observing planet f at the conjunction (the host can hinder the view) is not considered, its directions seen from planet e at this date and the date T_f apart at its opposition are almost parallel so that their intersection point approaches infinity (gray dots in Figure 11), leading to a failure of triangulation. The method of triangulation even gets more restricted when applied to planets g and h. Because T_g and T_h are nearly double and triple T_e, respectively, at the dates T_g or T_h apart, not only the planet observed but also planet e is in the same position so that no triangle can be formed. This obstacle to constructing the orbits of planets is hardly noticed in the solar system.

Nevertheless, we can still fit the most portion of the orbit of TRAPPIST-1f with an ellipse. The semimajor of planet f is fitted to be 1.3160 (scaled to the semimajor of planet e as Kepler scaled the solar system with 1 au), with an error of only 0.02%. However, the eccentricity is fitted to be 0.0109, 34% larger than the accurate value 0.0081 in that duration. The error of eccentricity can be as large as 100% when adopting data at other dates, revealing another obstacle. While the discovery of Kepler's first law is partly owed to the relatively high eccentricity of Mars in the solar system, the planets in the TRAPPIST-1 system all have very low eccentricities (Table 1),
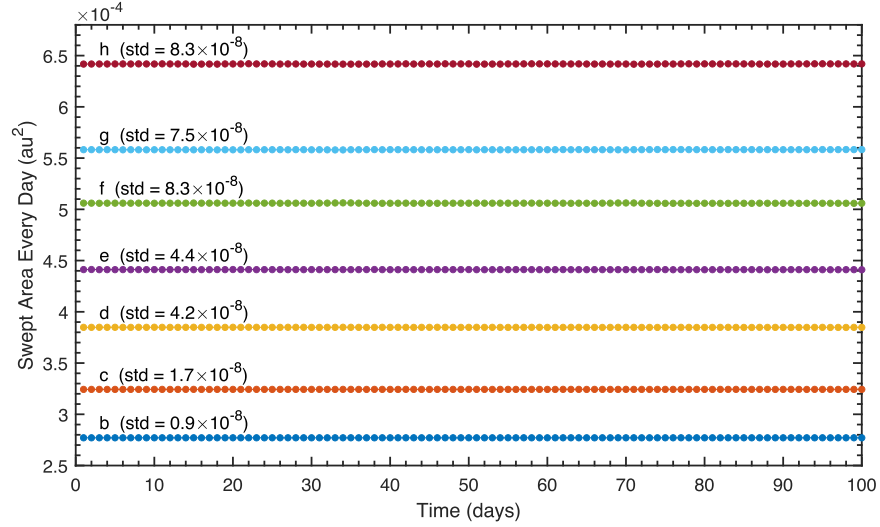
Figure 12. A comparison of the areas swept by planets in the TRAPPIST-1 system every day. The time origin is set as BJD = 2457257.931.
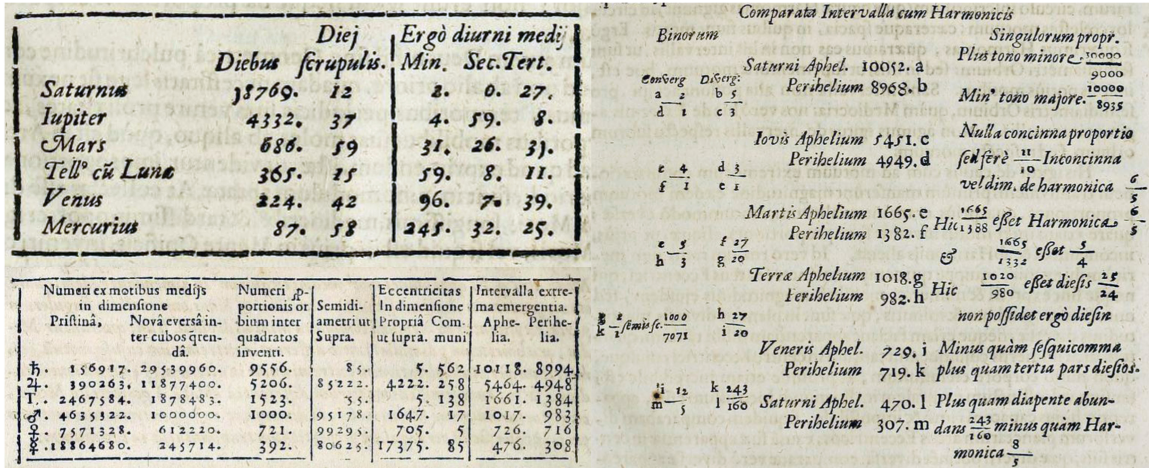

Figure 13. Orbital data from Harmonices Mundi (Kepler et al. 1619). Top left: orbital periods of six planets in the solar system; Bottom left: Kepler's harmonic universe theory and differences to real data; Right: perihelion and aphelion data for the six planets in the solar system.

resulting in great error of fitted eccentricity. The high precession rate which makes the orbit non-elliptical may also contribute to the error. The small orbital period allowing a short duration for observation partly compensates for it. Still, the orbit orientation of planet f changes by ~0°.1 during the observation time (based on the orbital evolution shown in Section 2), two orders of magnitude larger than that of Mars (Kahan et al. 2021).

Therefore, the low eccentricities, resonance chain and possibly fast precession in the TRAPPIST-1 system can make Kepler's first law quite hard to discover by triangulation. Still, the semimajor axes of planets can be precisely determined and the relative scale of the whole system can be realized, which helps the development of Kepler's second and third laws.

4.2. Kepler's Second and Third Laws

Kepler's second and third laws are both based on the determination of planets' distances to the Sun. Although Kepler's triangulation method can only determine the relative scale of the TRAPPIST-1 system (Section 4.1), the transit event allows the measurement of the absolute distance of TRAPPIST-1e to the host (Section 3.3). Thus, we consider it realistic to use the planets' absolute distances or semimajor axes to test the following two laws.

Kepler's second law states that a line connecting any planet and the Sun sweeps out equal areas in equal lengths of time (Kepler 1609). To validate Kepler's second law, we obtain both the position and velocity vectors in heliocentric coordinates from numerical integration (simulation in 100 days with an

Table 5.
Kepler's Calculation of the Constant of Kepler's Third Law in Harmonices Mundi and their Errors

	Mercury	Venus	Earth	Mars	Jupiter	Saturn
T_k (days)	87.58	224.42	365.25	686.59	4332.37	10769.12
T_a (days)	87.95	224.71	365.26	686.97	4332.67	10759.36
a_k (au)	0.3885	0.7240	1	1.5235	5.200	9.510
a_a (au)	0.3871	0.7233	1	1.5237	5.203	9.583
$C_k(10^{-6}\ \mathrm{au}^3\ \mathrm{day}^{-2})$	7.6447	7.5352	7.4917	7.5012	7.4913	7.4300
$C_a(10^{-6}\ \mathrm{au}^3\ \mathrm{day}^{-2})$	7.4983	7.4952	7.4956	7.4952	7.5048	7.6010
$C_{G\mu}(10^{-6}\ \mathrm{au}^3\ \mathrm{day}^{-2})$	7.4959	7.4959	7.4959	7.4959	7.5030	7.4980
Relative errors	1.72%	0.26%	−0.32%	−0.19%	−0.32%	−1.14%
Absolute errors	1.99%	0.52%	−0.06%	0.07%	−0.16%	−0.91%

Note. Constant C is calculated by different data. Subscript k stands for Kepler's data, and subscript a stands for accurate modern data (Til 2014). The relative errors are the deviations of each C_k from the C_k average of all six planets, while absolute errors are differences of C_k from the theoretical constant $C_{G\mu}$.

Table 6.
Kepler's Third Law Tested by the Inner Planets of the TRAPPIST-1 System

	TRAPPIST-1b	TRAPPIST-1 c	TRAPPIST-1d	TRAPPIST-1e
a_o (au)	0.01154	0.01580	0.02226	0.02929
a_a (au)	0.01155	0.01583	0.02229	0.02929
T_o (days)	1.501	2.413	4.029	6.052
T_a (days)	1.514	2.427	4.056	6.110
$C_o(10^{-7}\ \mathrm{au}^3\ \mathrm{day}^{-2})$	6.8298	6.7756	6.7963	6.8644
$C_a(10^{-7}\ \mathrm{au}^3\ \mathrm{day}^{-2})$	6.7313	6.7339	6.7347	6.7338
$C_{G\mu}(10^{-7}\ \mathrm{au}^3\ \mathrm{day}^{-2})$	6.7273	6.7273	6.7271	6.7271
Relative errors	0.19%	−0.60%	−0.30%	0.70%
E_{o-a}	1.46%	0.62%	0.91%	1.94%
$E_{o-G\mu}$	1.52%	0.72%	1.03%	2.04%

Note. Constant C are calculated via different data. Subscript a stands for accurate data calculated from numerical simulation, subscript o stands for observational data on planet e, and subscript Gμ stands for the theoretical constant calculated with $G(M_* + M_p)$. The relative errors are the deviations of each C_o from the C_o average of all four planets, while E_{o-a} and $E_{o-G\mu}$ represent the differences of C_o from C_a and $C_{G\mu}$, respectively.

integration step of 1/2000 days). By simulating the orbital motions of the seven planets, we obtain the areas swept every 1 day by each of the planets, as shown in Figure 12. The relative variations between the swept areas obtained over different times have magnitudes between 10^{-4} and 10^{-5}. This illustrates that in the TRAPPIST-1 system, Kepler's second law can still be discovered and validated precisely over short timescales, e.g., 100 days.

In Kepler's book, Harmonices Mundi (Kepler et al. 1619), he proposed his third law in Chapter 5, after describing the similar pattern of normal phenomenon and harmony of musical notes. The general form of Kepler's third law can be expressed as

$$\frac{a^3}{T^2} = C, \qquad (4)$$

where T is the orbital period and C is a constant for all planets in the solar system. The original data in the book are shown in Figure 13, which shows that its measurements of the semimajor axes and periods of the planets are only slightly different from

the modern values (Table 5). After converting the original data into modern units, we list Kepler's calculation results in Table 5. It can be seen that the main error in Kepler's calculation is due to uncertainty in the semimajor axis.

Using an expression similar to Kepler's in the book (Figure 13), we list the semimajor axes and orbital periods of planets in the TRAPPIST-1 system in Table 6. All the accurate semimajor axes or orbital periods are the averages of simulated values in 100 days. The observed semimajor axis of planet e is set as the same as the accurate value 0.02929 au. The other planets' observed semimajor axes are obtained by Kepler's triangulation method (Section 4.1) and then scaled to their absolute values. The observed period of planet e is the length of time the host takes to return to the same apparent position in the sky, while the other planets' observed periods are determined by the time between two successive transits.

As can be seen from Table 6, the data observed on TRAPPIST-1e basically supports the validation of Kepler's third law. The observed gravity constants C_o are consistent
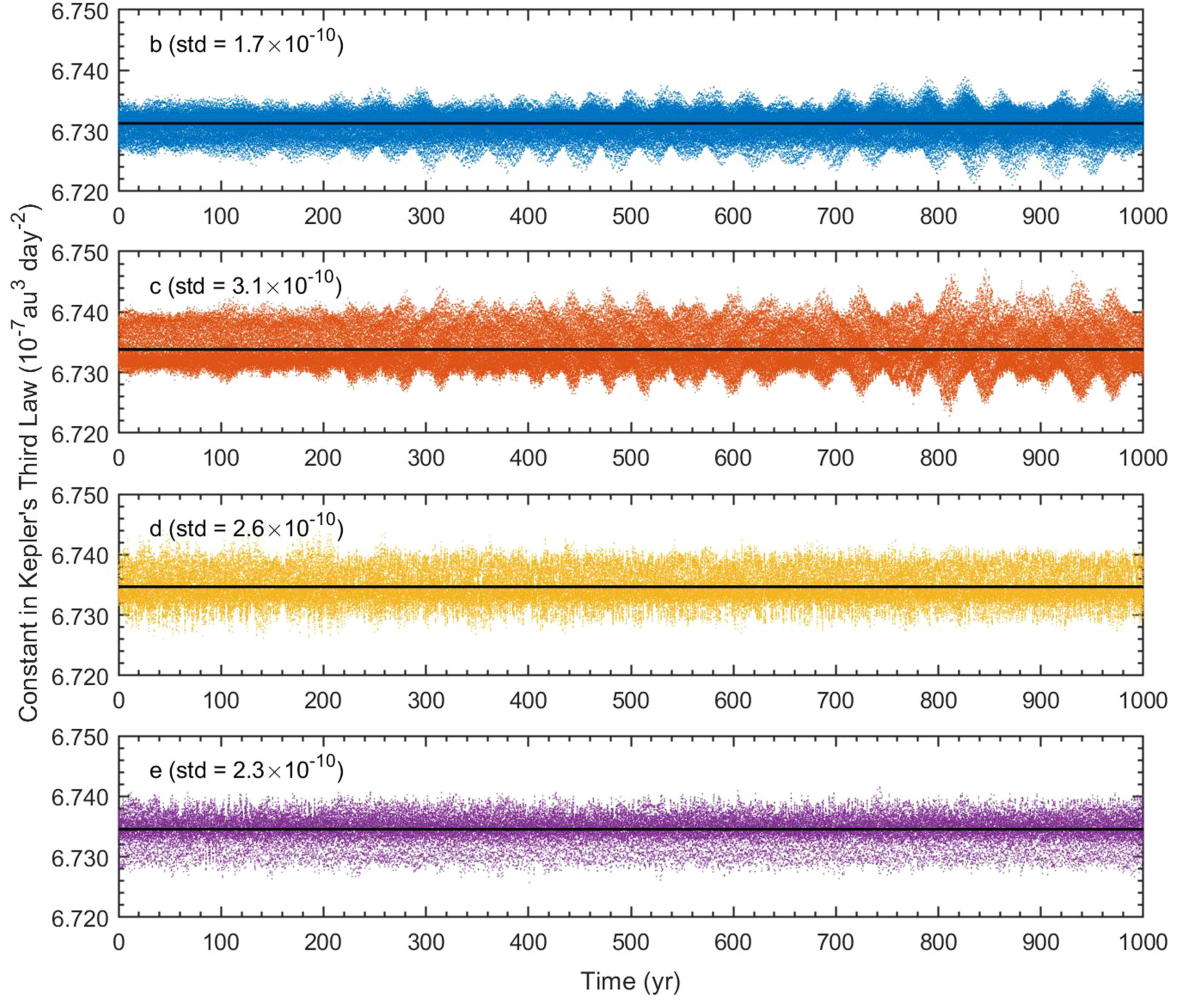
Figure 14. Variation of the constant in Kepler's third law of planets b, c, d, and e in 1000 yr since 2457257.931 BJD, derived from simulated orbital evolutions in Section 2. Black lines are the averages of constants.

with theoretical values $C_{G\mu}$ with differences of no more than about 2%. Compared to Kepler's data of the solar system, the absolute errors of semimajor axes in the TRAPPIST-1 system are smaller. The constants C_k obtained by Kepler deviate from the theoretical values $C_{G\mu}$ by no more than 2%, the same amount as that in the TRAPPIST-1 system, although the deviation is smaller for planets near Earth. In addition, the deviation from 2-body motion caused by the gravitational perturbations E_{o-a} is smaller than anticipated in such a compact system. Figure 14 further shows that on longer timescales like 1000 yr, the variation of the simulated Kepler constant C_a stays no greater than 0.05%, which is much less than the observational error E_{o-a}. In brief, the Kepler constant deviates from theoretical values due to both gravitational perturbations and observational error. Since the deviation is at a magnitude of 1%, we can still conclude that Kepler's third law can be proven in the TRAPPIST-1 system.

4.3. Great Inequality Disobeying Kepler's Laws

The extensive research on the Great Inequality is an indispensable chapter in the development of celestial mechanics, which has let astronomers explicitly understand the motion of celestial bodies and the stability of the solar system (Wilson 1985). Briefly, the Great Inequality refers to the deviation from the empirical predictions and even ephemeris derived from Kepler's law or Newton's universal gravity theory before the 18th century. Extraordinary astronomers like Kepler and Halley observed that Jupiter always accelerates while Saturn decelerates, misleading to an alarming prediction that Jupiter would fall into the Sun and Saturn would be driven away. To avoid these disasters and to confirm the stability of our solar system, many outstanding scientists have tried to reconcile this paradox. Euler and Lagrange introduced trigonometric functions into the calculation of perturbation, which made the analytical solution possible.

Eventually, Laplace (1785) and Lagrange (1776) solved the problem by adding high-order perturbations between the planets and interpreting the Great Inequality as a 5:2 resonance between Saturn and Jupiter. They derived from energy conservation that

$$\sum_j \frac{M_j}{a_j} = \text{Constant}. \tag{5}$$

The other planets in the solar system can be ignored in the equation. Given Kepler's third law, this implies

$$\frac{\Delta n_{\text{Sat}}}{\Delta n_{\text{Jup}}} = -\frac{M_{\text{Jup}}}{M_{\text{Sat}}}\sqrt{\frac{a_{\text{Jup}}}{a_{\text{Sat}}}} = -2.47, \tag{6}$$

(calculated with modern values of planet parameters) where Δn is the deviation of mean motion from the unperturbed elliptical motion.

The research process of the Great Inequality is quite an excellent saga. In this work, we consider if such a problem would impact the observers on TRAPPIST-1e. In the TRAPPIST-1 system, planets b, c, f and g all have masses slightly more than 1 $M_\oplus$ and are in a long resonance chain. Therefore, it is not as realistic as the solar system to estimate the ratio of mean motion deviations of two planets exclusively. Accounting for this, we derive the theoretical ratios $\Delta n_c/\Delta n_b = -0.90$ and $\Delta n_g/\Delta n_f = -0.71$ from the mean semimajor axes in the simulation to compare with the simulated ratios. They are closer to 1 than $\Delta n_{\text{Sat}}/\Delta n_{\text{Jup}}$. We focus on those pairs of planets to check if the Great Inequality is noticeable.

The simulated mean motion deviations (mean motions calculated with simulated orbital periods and then subtracted by the averages) are illustrated in Figure 15. A negative correlation between planets b and c is visible over 0–1000 yr and their deviations stay at nearly the same level. The average ratio of smoothed deviation $\Delta n_c/\Delta n_b$ over this time is -0.69, comparable to its theoretical estimate. We attribute this rough consistency to their portions in the lead of items in Equation (5) due to the shortest semimajor axes as well as their masses. As for the pair of planets f and g, the correlation is more complex. A slice of 2500–3500 yr from the whole simulation is taken as an example in Figure 15. In general, planets f and g exhibit a negative correlation, which is the most obvious from about 2740 to 3040 yr. However, their deviations do not keep a consistent proportion from decade to decade, e.g., the ratio $\Delta n_g/\Delta n_f$ around the year 2600 is apparently lower than the following years around 2660. Meanwhile, as the outermost planet whose mass 0.326 $M_\oplus$ is one magnitude smaller than its neighbors, planet h occasionally shows a negative correlation with g before 2700 yr and after 3400 yr, when that correlation between planets f and g becomes ambiguous. The average ratio of smoothed deviation $\Delta n_g/\Delta n_f$ over this time is -1.41, nearly double that of its theoretical estimate. We also calculate the correlation coefficient between the smoothed mean motion

deviations to verify the negative correlations. Over those selected times in Figure 15, the correlation coefficient between planets b and c is -0.74, whereas that between f and g is -0.59, though they both turn out milder over the whole 5 kyr, i.e., -0.69 and -0.46.

Though the clues to the Great Inequality are present in the TRAPPIST-1 system, it has to be made clear that this phenomenon is more elusive than in the solar system. Because TRAPPIST-1 is more compact and has multiple planets with comparable masses, contrary to the dominance of Jupiter and Saturn in the solar system, the accompanying deceleration and acceleration can transfer to different pairs of planets at different times. The potential civilization on TRAPPIST-1e may need to take more than two planets into account at the same time to confirm energy conservation (Equation (5)), giving rise to a higher requirement for observations. Nevertheless, within ~100 yr when the Great Inequality is stable between some pairs of planets, probably the planets b and c, there is still a chance to spot this phenomenon and trigger exploration.

5. Perihelion Precession due to General Relativity

In Section 4, we verified Kepler's laws in the TRAPPIST-1 system based on Newtonian mechanics. At the beginning of the 20th century, Einstein developed the theory of special relativity and general relativity (Einstein 1905, 1915). From astronomical observations in the next few decades, Einstein's theory was validated by the observed perihelion precession of Mercury (Nobili & Will 1986), as well as gravitational lensing events (Walsh et al. 1979) and gravitational waves (Abbott et al. 2016, 2017).

In this section, we will focus on the perihelion precession of inner planets (i.e., planets b, c and d) to test the effects due to general relativity (hereafter GR) and the observability in TRAPPIST-1 system. Taking the perturbations of GR into consideration, the perihelion shift caused by relativity can be expressed as (Wu & Goldreich 2002; Earman et al. 1993)

$$P_{\text{GR}} = 3n\frac{GM_*}{ac^2(1 - e^2)}, \tag{7}$$

where P_{GR} represents the perihelion precession rate $d\omega/dt$ caused by relativity precession, n is the mean motion of the planet and c is the light speed. Thus, we can calculate the rate of perihelion precession of each planet via Equation (7). Meanwhile, simulated data in Section 2 provides the perihelion precession due to the gravity of other planets P_g. Given the complex dynamics of the system, a slice of 1500–2000 yr from the whole simulation, a typical period when the precession rates of inner planets are relatively stable, is selected to derive P_g in Table 7.

Table 7 shows that the precession of inner planets is dominated by gravitational perturbations, while relativity effects contribute ~0.1% of the total procession rate. The
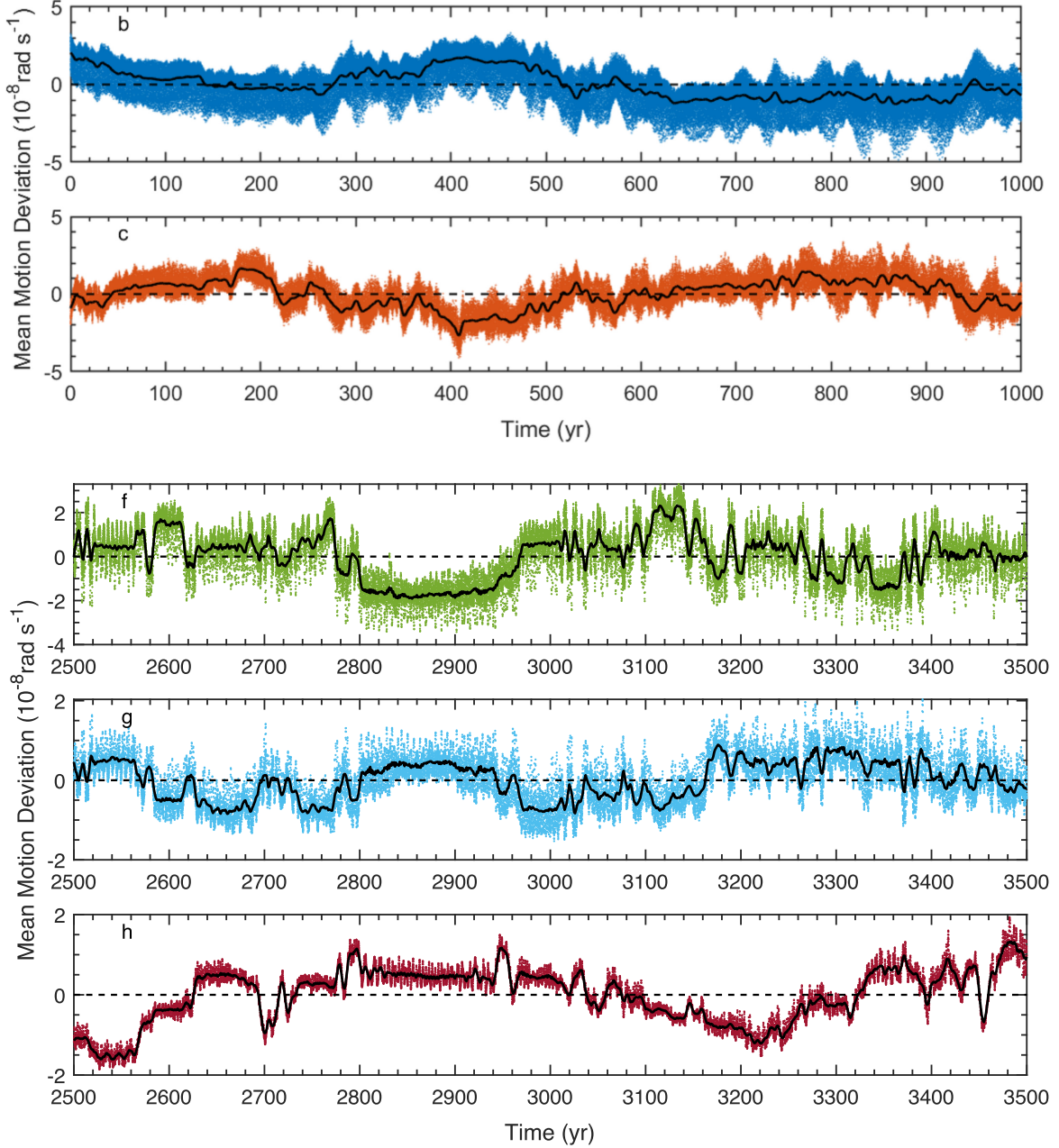
Figure 15. Mean motion deviations from averages over 0–1000 yr for planets b and c and 2500–3500 yr for planets f, g, and h in the TRAPPIST-1 system. The black curves indicate the smoothed mean motions, and the black dashed lines indicate the mean motion averages.

gravitational precession P_g of planets b and c is quite close and both are fast in the order of $100'' \, day^{-1}$, and planet d is slightly slower with the rate of $71'' \, day^{-1}$. The GR precession rate P_{GR} of the innermost planet b is the largest, $0''.197 \, day^{-1}$, while planet d has the smallest rate at $0''.038 \, day^{-1}$. Compared to Mercury, although the GR precession rate of planets b, c, and d are 1–2 orders of magnitude larger, the gravitational precession in the TRAPPIST-1 system is even 3–4 orders of magnitude

larger than Mercury due to the compactness. Thus the relative contribution of GR, P_{GR}/P_g is no more than ~0.1% for all the three inner planets in TRAPPIST-1, dozens of times smaller than that of Mercury, 8.1%. The pericenter precession rate caused by GR in TRAPPIST-1 is insignificant.

Because the inner planets in the TRAPPIST-1 system are much closer to their host star than Mercury (indicating a stronger tidal effect), the perihelion precession due to tides of

Table 7
The Pericenter Precession Rate of the Inner TRAPPIST-1 Planets and Mercury (Clemence 1947) Caused by Different Effects

	TRAPPIST-1b	TRAPPIST-1 c	TRAPPIST-1d	Mercury
P_{GR} ($''$ day^{-1})	0.197	0.090	0.038	1.18×10^{-3}
P_g ($''$ day^{-1})	103	102	71	0.0146
P_t ($''$ day^{-1})	4.99×10^{-2}	6.22×10^{-3}	4.33×10^{-4}	3.50×10^{-11}
P_{GR}/P_g	0.19%	0.09%	0.05%	8.1%
P_{GR}/P_t	3.94	14.4	88.0	3.36×10^7

Note. Subscript GR stands for general relativity, g stands for gravity, and t stands for tidal effect.

the host star needs to be considered. We use the formula below to calculate the precession speed due to the tidal effect (Wu & Goldreich 2002):

$$P_t = 7.5nk\frac{1 + 3e^2/2 + e^4/8}{(1 - e^2)^5}\frac{M_*}{M_p}\left(\frac{R_p}{a}\right)^5 \qquad (8)$$

Here k is the Love number, describing the elasticity of a planet with no dimension (Love 1911). For terrestrial planets, k can be set as 0.3 (Dong & Ji 2013). We thus calculate the tidal effect of planets b, c and d, as shown in Table 7.

We can see that the effect of tides on the precession of the TRAPPIST-1 planets, P_t, are at least 10^7 times stronger than Mercury, but still, all the tidal effects are weaker than relativity, not to mention gravity. For the innermost planet b, GR is about 4 times the tidal effect. As the distance to the host star gets larger, the tidal effect decreases more rapidly than the GR effect because of its distance-sensitive property, leading to the ratio of precession rates due to GR and tides, P_{GR}/P_t, fast increasing. This ratio increases to 88 for planet d.

We further generalize this calculation of P_{GR}/P_t to planets of different masses in nearly circular orbits with the distance from the host star varying. Figure 16 shows an apparent positive correlation between this ratio and the semimajor axis of a planet, regardless of the mass of the host the planet is orbiting. The GR effect is greater than the tidal effect for a terrestrial planet of one Earth-mass as long as a is greater than 0.0077 au. A bigger mass for the planet decreases the ratio by strengthening tides, which is still exceeded by GR for a compact system like TRAPPIST-1. Therefore, tides can usually be neglected compared to the GR effect.

Considering that the gravitational precession rate is enhanced more significantly than the GR effect in the TRAPPIST-1 system, despite the relatively weaker and even negligible tides, the GR effect can hardly be verified by observing the pericenter precession of inner planets.

6. Conclusion

In this paper, we produce planet ephemeris in the typical compact multiple planetary system around an M dwarf, TRAPPIST-1, and test the precision of measuring gravity theory. In Section 2, we simulate the TRAPPIST-1 system over
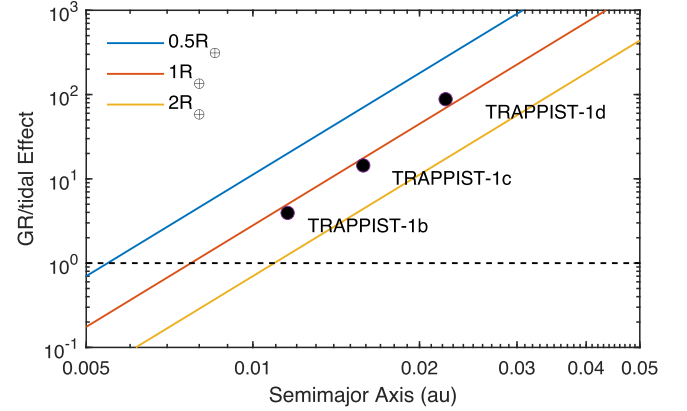

Figure 16. The ratio of precession rates of pericenter due to the general relativity and the tidal effect. The lines represent the ratio for planets in circular orbits ($e = 0$) with different masses (0.5, 1, and 2 Earth radii times Earth's density) around a host star (whose mass does not influence the theoretical estimate of the ratio). Circles indicate three inner planets in the TRAPPIST-1 system.

5 kyr (Figure 1) and establish a planetary ephemeris for planet e. The evolution of the orbital elements of the seven planets is stable at the timescale of 1 Myr (Figure 2) despite the complex dynamics of such a compact system.

In Section 3, we first validate the present-day synchronous status of planet e via its short damping timescale of 1 kyr. Its spin evolution leads to its insolation close to Earth as support for habitability and then used to produce the retrograde motions of other planets in the horizontal coordinates of planet e. The retrograde motions seen from planet e show different characteristics from the solar system due to the compactness, including smaller duration and interval, and much higher frequency (Table 4). We also simulate the transit events of three inner planets occurring in TRAPPIST-1, which are needed to estimate the semimajor axes of these planets when Kepler's Law is tested (Section 4).

In Section 4, we test Kepler's laws and the Great Inequality in the TRAPPIST-1 system. The triangulation method for constructing orbits results in fitting errors of eccentricities being several tens of percent, but with those of semimajor axes only $\lesssim$0.1%. The swept area of each planet in the simulation turns out to be quite stable on a short timescale of hundreds of

days (Figure 12). With observation accuracy of ~1% (Table 5), similar to Kepler's calculation of the solar system, the constant of Kepler's third law in TRAPPIST-1 varies within ~0.01% on a timescale of 10^3 yr (Figure 14). Therefore, we conclude that though Kepler's first law is hard to verify for the low eccentricities in the TRAPPIST-1 system, Kepler's second and third laws can still be developed in such a compact system. In addition, correlations between the mean motions of planets indicate that the Great Inequality is elusive in TRAPPIST-1, though the accompanying deceleration and acceleration of planets b and c are relatively visible.

In Section 5, we test GR. The pericenter precession rates due to GR of the inner planets in the TRAPPIST-1 system are bigger than that of Mercury, but the contributed fractions due to the GR effect are only dozens of times smaller than Mercury (Table 7). Thus, although the tidal effects acting on these planets are weak relative to GR, the probability for intelligence on TRAPPIST-1e to discover this phenomenon is largely weakened.

In summary, the multi-planetary systems around M stars are usually compact and do suffer from stronger gravitational perturbation, but in the TRAPPIST-1 system, this effect does not block potential civilizations from discovering basic gravitational laws, e.g., heliocentric theory and Kepler's Laws. However, the resonant chain in such compact systems is complex, so we do not eliminate the possibility that Kepler's first law and GR are hidden in secular chaotic dynamical evolution.

Acknowledgments

ORCID iDs

Nan Wang ⬤ https://orcid.org/0000-0002-8459-8067

References

A Society of Gentlemen in Scotland 1771, in Encyclopaedia Britannica, ed. W. Smellie, Vol, 1 (Edinburgh: Andrew Bell and Colin Macfarquhar), 434
Abbott, B. P., Abbott, R., Abbott, T. D., et al. 2016, PhRvL, 116, 061102
Abbott, B. P., Abbott, R., Abbott, T. D., et al. 2017, PhRvL, 119, 161101
Adams, J. C. 1846, MNRAS, 7, 149
Agol, E., Dorn, C., Grimm, S. L., et al. 2021, PSJ, 2, 1

Anand, M., Aschwanden, M., Bagenal, F., et al. 2014, in Encyclopedia of the Solar System, ed. T. Spohn, D. Breuer, & T. Johnson (3; Boston: Elsevier), 1235
Bolmont, E., Raymond, S. N., Leconte, J., Hersant, F., & Correia, A. C. M. 2015, A&A, 583, A116
Borucki, W. J., Koch, D., Basri, G., et al. 2010, Sci, 327, 977
Browne, L. W. B. 2005, AHES, 59, 251
Chambers, J., Wetherill, G., & Boss, A. 1996, Icar, 119, 261
Clemence, G. M. 1947, RvMP, 19, 361
Pappus, A., Commandino, F., & Aristarchus 1572, Aristarchi De Magnitudinibus, et Distantiis Solis, et Lunae, Liber, cum Pappi Alexandrini Explicationibus Quibusdam. (Pisauri: apud Camillum Francischinum),
Copernicus, N. 1543, De Revolutionibus Orbium Coelestium (Norimbergae: Apud J. Petreium),
Dong, C., Jin, M., Lingam, M., et al. 2018, PNAS, 115, 260
Dong, Y., & Ji, J. 2013, MNRAS, 430, 951
Ducrot, E., Gillon, M., Delrez, L., et al. 2020, A&A, 640, A112
Earman, J., Janssen, M., & Norton, J. D. 1993, The Attraction of Gravitation: New Studies in the History of General Relativity, Vol. 5 (Boston: Birkhuser),
Eggleton, P. P., Kiseleva, L. G., & Hut, P. 1998, ApJ, 499, 853
Einstein, A. 1905, AnP, 322, 891
Einstein, A. 1915, SPAW, 47, 831
Gillon, M., Triaud, A. H. M. J., Demory, B.-O., et al. 2017, Nature, 542, 456460
Gizis, J. E., Monet, D. G., Reid, I. N., et al. 2000, AJ, 120, 1085
Halley, E. 1716, RSPT, 29, 454
Heising, M. Z., Sasselov, D. D., Hernquist, L., & Humphrey, A. L. T. 2021, ApJ, 913, 126
Helden, A. V. 1985, Measuring the Universe: Cosmic Dimensions from Aristarchus to Halley (Chicago: Univ. Chicago Press)
Herschel, W., & Watson, D. 1781, RSPT, 71, 492
Hill, M. L., Bott, K., Dalba, P. A., et al. 2023, AJ, 165, 34
Hornsby, T. 1771, RSPT, 61, 574
Izidoro, A., Bitsch, B., Raymond, S. N., et al. 2021, A&A, 650, A152
Jehin, E., Gillon, M., Queloz, D., et al. 2011, Msngr, 145, 2
Ji, J.-H., Li, H.-T., Zhang, J.-B., et al. 2022, RAA, 22, 072003
Joshi, M. 2003, AsBio, 3, 415
Kahan, D. S., Folkner, W. M., Buccino, D. R., et al. 2021, P&SS, 199, 105208
Kepler, J. 1609, Astronomia nova ..., seu physica coelestis, tradita commentariis de motibus stellae martis (Heidelberg: Voegelin),
Kepler, J. 1627, Tabvlae Rudolphinae, qvibvs astronomicae scientiae, temporum longinquitate collapsae restauratio continetur (Ulm: T. Saurii)
Kepler, J., Ptolemaeus, C., & Fludd, R. 1619, Harmonices mvndi libri v. qvorvm primus geometricvs, de figurarum regularium, quae proportiones harmonicas constituunt, ortu & demonstrationicvs, secundus architectonicvs, SEU EX geometria figvrata, de figurarum regularium congruentia in plano vel solido: tertius proprie harmonicvs, de proportionum harmonicarum ortu EX figuris (Lincii Austriae),
Lagrange, J.-L. 1776, Sur l'altération des moyens mouvements des planètes, Mémoires de l Académie de Berlin, 199 Oeuvres complétes VI 255 Gauthier-Villars) (Paris:
Laplace, P. S. 1785, Mémoires de l'Académie royale des sciences de Paris, 11, 95
Le Verrier, U. J. 1846a, AN, 25, 65
Le Verrier, U. J. 1846b, AN, 25, 53
Love, A. E. H. 1911, Some Problems of Geodynamics (Cambridge: Cambridge University Press),
Lu, T., Rein, H., Tamayo, D., et al. 2023, ApJ, 948, 41
Luger, R., Sestovic, M., Kruse, E., et al. 2017, NatAs, 1, 0129
Mann, A. W., Dupuy, T., Kraus, A. L., et al. 2019, ApJ, 871, 63
Newton, I. 1687, Philosophiae Naturalis Principia Mathematica (London: Jussu Societatis Regiae ac Typis Josephi Streater ...),
Nobili, A. M., & Will, C. M. 1986, Natur, 320, 39
Otegi, J. F., Bouchy, F., & Helled, R. 2021, Similarity of multi-planetary systems, in Posters from the TESS Science Conf. II (TSC2), 44
Rein, H., & Liu, S. F. 2012, A&A, 537, A128
Rein, H., & Spiegel, D. S. 2015, MNRAS, 446, 1424

Ricker, G. R., Winn, J. N., Vanderspek, R., et al. 2015, JATIS, 1, 014003
Schoonenberg, D., Liu, B., Ormel, C. W., & Dorn, C. 2019, A&A, 627, A149
Segura, A., Walkowicz, L. M., Meadows, V., Kasting, J., & Hawley, S. 2010, AsBio, 10, 751
Short, J. 1761, RSPT, 52, 611
Short, J. 1763, RSPT, 53, 300
Tamayo, D., Rein, H., Petrovich, C., & Murray, N. 2017, ApJL, 840, L19
Tamayo, D., Rein, H., Shi, P., & Hernandez, D. M. 2020, MNRAS, 491, 2885
Teets, D. 2003, Mathematics Magazine, 76, 335

Tilley, M. A., Segura, A., Meadows, V., Hawley, S., & Davenport, J. 2019, AsBio, 19, 64
Toomer, G. J. 1978, Hipparchus, Dictionary of Scientific Biography, 15, 207
Volk, K., & Malhotra, R. 2020, AJ, 160, 98
Walsh, D., Carswell, R. F., & Weymann, R. J. 1979, Natur, 279, 381
Wang, N., & He, Z.-G. 2019, RAA, 19, 122
Weiss, L. M., Marcy, G. W., Petigura, E. A., et al. 2018, AJ, 155, 48
Wilson, C. 1985, AHES, 33, 15
Wolf, E. T. 2017, ApJL, 839, L1
Wu, Y., & Goldreich, P. 2002, ApJ, 564, 10241027